

Idler-resonant optical parametric oscillator based on KTiOAsO_4

Fen Bai · Qingpu Wang · Zhaojun Liu ·
Xingyu Zhang · Weixia Lan · Xutang Tao ·
Youxuan Sun

Received: 7 December 2012 / Accepted: 5 March 2013 / Published online: 26 March 2013
© Springer-Verlag Berlin Heidelberg 2013

Abstract An idler-resonant KTiOAsO_4 (KTA) optical parametric oscillator is demonstrated within a diode-end-pumped acousto-optically Q-switched Nd:YAG laser. With an X-cut KTA crystal, idler wave at 3467 nm and signal wave at 1535 nm are generated. Under an incident diode pump power of 15.4 W, the idler output power of 105 mW and signal power of 720 mW are obtained at a pulse repetition rate of 40 kHz. The pulse widths of the idler and signal waves are 7.2 and 3.1 ns, respectively. The beam quality factors (M^2) of the idler wave are within 1.2 in both horizontal and vertical directions.

1 Introduction

Radiation with good beam quality in mid-infrared (mid-IR) (3–5 μm) spectral region has many interesting applications such as radar, telemetry, remote sensing, biomedicine, etc. Frequency conversion through optical parametric oscillators (OPOs) is an effective method to generate radiations in this band [1–14]. Many nonlinear crystals are chosen in mid-IR OPOs. One kind of the nonlinear crystals are those

periodically poled crystals, such as PPLN (Periodically Poled LiNbO_3), PPKTP (Periodically Poled KTiOPO_4), PPSLT (Periodically Poled LiTaO_3), etc. Recently, Gaydardzhiev et al. [11] reported a high pulse energy and high average power mid-IR OPO based on PPSLT. Another kind of crystals, such as ZnGeP_2 (ZGP), AgGaS_2 , LiInSe_2 , and CdSiP_2 , are also employed to realize mid-IR OPOs. For example, Dergachev et al. [12] achieved 3.4 μm radiation with pulse energy of 10 mJ with a ZGP nanosecond OPO. KTiOPO_4 (KTP) and its isomorphs have also been widely used in OPOs for many advantages, such as large nonlinear coefficient, high optical damage threshold and commercial availability [15, 16]. Compared with KTP, KTiOAsO_4 (KTA) has higher transmission in the 3–5 μm region and does not have the absorption feature seen in KTP near 3.47 μm . This makes KTA more attractive than KTP in high power mid-IR OPOs [2–8, 13, 14]. Wu et al. [2] achieved 4.1 W at 3.5 μm output and 15 W total output from a KTA-OPO pumped by Nd:YALO laser. Zhong et al. [6] achieved 31 mJ output energy at 3.47 μm from a side-pumped electrooptical (EO) Q-switched Nd:YAG laser. In these KTA-OPOs, widely used 1 μm lasers were used as the pumping source. Employing the type II noncritical phase matching (NCPM) scheme, KTA generated 1.5 μm eye-safe and 3.5 μm mid-IR radiations simultaneously. As defined traditionally, the two waves from OPO are called *signal* and *idler* waves for the high and low frequency ones, respectively. So in this work, we denote 1.5 μm wave as signal and 3.5 μm wave as idler. As far as we know, all the previous KTA-OPOs were configured that 1.5 μm waves (signal) were resonated and the 3.5 μm ones (idler) were not. As a result, the beam quality factors of the 3.5 μm waves were much larger than the signal [2, 3, 8].

To improve the beam quality of 3.5 μm wave, people propose an idea of developing an idler-resonant OPO.

F. Bai · Q. Wang (✉) · Z. Liu · X. Zhang · W. Lan
School of Information Science and Engineering and Shandong
Provincial Key Laboratory of Laser Technology
and Application, Shandong University, Jinan,
Shandong 250100, People's Republic of China
e-mail: qpwang@sdu.edu.cn

Q. Wang
Advanced Research Center for Optics, Shandong University,
Jinan, Shandong 250100, People's Republic of China

X. Tao · Y. Sun
State Key Laboratory of Crystal Materials, Shandong University,
Jinan, Shandong 250100, People's Republic of China

However, it is not easy to realize such a device. Firstly, the pumping intensity has to be high enough to reach the oscillating threshold for OPO. According to the theoretical analysis, the OPO threshold is increasing with resonated wave shifting to longer wavelength [17]. So for idler-resonant OPO, the oscillating threshold is higher than that for signal-resonant one. Secondly, a low-loss OPO resonator is necessary. All the elements inside the OPO resonator are required to have low-absorption coefficient at idler wavelength, i.e., 3.5 μm in this work. Thirdly, it is difficult to prepare the highly reflectivity (HR) dielectric multilayer mirror coatings with high damage threshold at mid-infrared region, especially for the coatings in intracavity configurations. These mirrors should be coated for high transmission at the pumping wavelength simultaneously.

In this paper, we present what are believed to be the first laboratory study of KTA-OPO with idler wave resonated. To produce high pump intensity, an efficient diode-end-pumped acousto-optical Q-switched Nd:YAG laser was used as the pumping source. And intracavity configuration was designed to take advantage of the high intensity inside the pumping laser cavity. To ensure a low-loss OPO resonator, we chose KTA crystals with high optical quality and the substrates of the OPO cavity mirrors were made of special materials which have high transmissions at 3.5 μm . One OPO cavity mirror was made of infrared silica glass (JGS3) and the other was made of Al_2O_3 material. To realize our idler-resonant intracavity OPO, we carefully designed the cavity mirror coatings for strongly resonant at 1.06 and 3.5 μm and non-resonant at 1.5 μm . The coating data would be described in detail below. As a result, 105 mW idler wave and 720 mW signal wave were obtained at an incident diode pump power of 15.4 W and a repetition rate of 40 kHz. The spectral, temporal and beam quality characteristics were analyzed for both signal and idler waves. The beam quality factors (M^2) of idler wave in two orthogonal directions were measured to be 1.1 ± 0.2 and 1.2 ± 0.2 .

2 Experimental setup

Experimental configuration is shown in Fig. 1. An 808 nm fiber coupled CW diode laser ($\text{NA} = 0.22$, $d_{\text{core}} = 600 \mu\text{m}$) was used to produce 1,064 nm wave. The laser gain medium was a 1 at.% Nd-doped YAG rod with a dimension of $\phi 4 \text{ mm} \times 10 \text{ mm}$. Both surfaces of Nd:YAG were anti-reflection (AR) coated at 808 and 1,064 nm ($R < 0.2 \%$). The pump beam was re-imaged into the laser crystal and the waist diameter was 600 μm . The KTA crystal with a size of $4 \times 4 \times 25 \text{ mm}^3$ was cut along its X -axis ($\theta = 90^\circ$, $\phi = 0^\circ$) to realize type II NCPM of $1,064 \text{ nm} \leftrightarrow 1,535 \text{ nm} + 3,467 \text{ nm}$. And its coating were

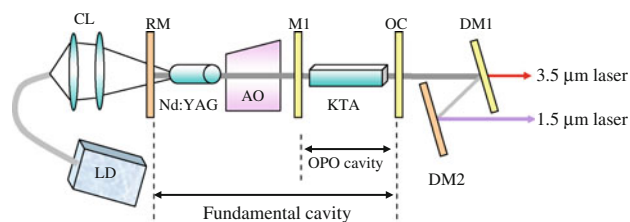


Fig. 1 Experimental setup for idler-resonant KTA-OPO. LD laser diode, CL coupling lens, RM rear mirror, OC output coupler, AO acousto-optical Q-switch, DM dichroic mirror

AR ($R < 0.2 \%$) at 1,064 and 1,535 nm and high transmission (HT) ($T > 95 \%$) at 3,467 nm on both surfaces. The 38-mm-long AO Q-switch (Gooch and Housego) had AR coatings ($R < 0.2 \%$) on both faces at 1,064 nm and was driven at 41 MHz center frequency with 15 W of rf power. The Nd:YAG, KTA and Q-switch were water cooled with the water temperature of 20 $^\circ\text{C}$.

The entrance face of the rear mirror (RM) was coated for AR at 808 nm ($R < 0.2 \%$). The other face was coated for high reflection (HR) at 1,064 nm ($R > 99.8 \%$) and HT at 808 nm ($T > 99 \%$). M1 was made of infrared silica glass (JGS3). Its one surface was coated for AR at 1,064 nm ($R < 0.2 \%$) and the other surface coated for HT at 1,064 nm ($T > 99.5 \%$) and HR at both 1,535 and 3,467 nm ($R > 99.8 \%$). A flat mirror made of Al_2O_3 was employed as output coupler (OC). It was coated for HR at 1,064 ($R > 99.9 \%$), partial reflection (PR) at 3,467 nm ($R = 91 \%$) and HT at 1,535 nm ($T > 99.3 \%$). Thus, the resonator was a singly resonant intracavity OPO. The 1.06 μm wave oscillated between RM and OC and 3.5 μm wave oscillated between M1 and OC. The generated 1.5 μm laser in both directions could be output. The overall cavity length was 96 mm and the OPO cavity length was 36 mm.

3 Results and discussions

In order to study the output characteristics of 1.5 and 3.5 μm waves, we prepared two dichroic mirrors (DMs). One (DM1) was made of CaF_2 and the other (DM2) made of conventional BK7 glass. DM1 was coated for HR at 1,535 and 1,064 nm and HT at 3,467 nm to separate 3.5 μm laser from the total output light. DM2 was coated for HR at 1,535 nm and HT at 1,064 nm to separate 1,535 nm laser from the residual fundamental laser.

We first studied the spectral characteristics of the output waves. The wavelengths of the fundamental and signal waves were monitored by a wide range spectrum analyzer (Yokogawa AQ6315A, 350–1,750 nm). The wavelengths were measured to be 1,064.2 and 1,535.5 nm for the fundamental and signal laser, respectively. The idler spectral

information was monitored with a spectral analyzer consisted of a monochromator, a pyroelectric detector and a data acquisition system. The scanned results from 3,410 to 3,500 nm are shown in Fig. 2, from which a central wavelength of 3,467 nm could be obtained.

The average output power characteristics were measured with an EPM 2000 power meter (Coherent Inc.). Figure 3 shows the average output power with respect to the diode pump power at pulse repetition rates (PRRs) of 20, 30, 40, and 50 kHz. Figure 3a, b, respectively, corresponds the results for 1.5 and 3.5 μm lasers. From these figures, we can see the OPO oscillation threshold at 20, 30, 40, and 50 kHz were 4.8, 5.7, 6.4, and 6.8 W, respectively. The output powers saturated and declined when pump powers were higher than certain values. The highest signal power was obtained to be 720 mW and idler power to be 105 mW at diode pump power of 15.4 W and PRR of 40 kHz. The conversion efficiency from the LD power to signal and idler power were 4.7 and 0.7 %. The main reason for such a low efficiency may lie in the randomly polarized 1,064 nm

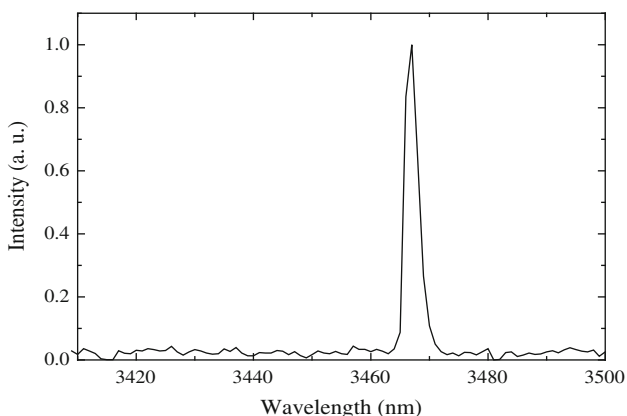


Fig. 2 Optical spectrum of idler wave from the KTA-OPO

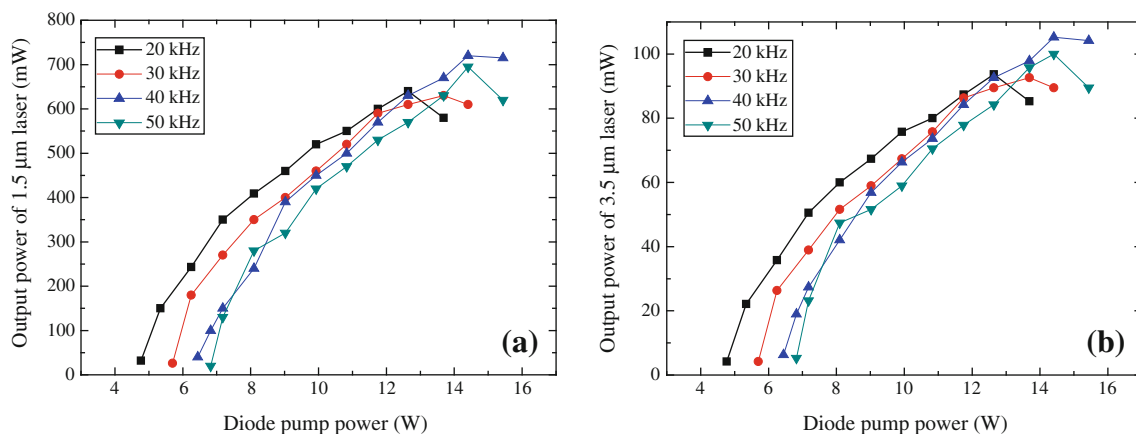


Fig. 3 Average output powers with respect to the diode pump powers for idler-resonant KTA-OPO. **a** 1.5 μm laser. **b** 3.5 μm laser

light produced from the isotropic Nd:YAG crystal. OPO process is dependent upon the polarization state of interacted radiations [18]. Only the photons with the “right” polarization can contribute to OPO gain. The photons with the “wrong” polarization were wasted and the conversion efficiency was limited. Using other material such as a-cut Nd:YVO₄ or Nd:YALO as the laser crystal to generate linear polarized fundamental laser, we expect to increase the OPO conversion efficiency. Moreover, the thermal effects of the crystals also influenced the OPO conversion efficiency. With the pump power increasing, the thermal effects were becoming more and more serious. The serious thermal focal lens effect would result in the instability of the resonator. So, the output power would decline when pump power was higher than certain value, as shown in Fig. 3. For the laser crystal, by selecting a diffusion-bonded crystal or increasing the pump beam size, the thermal load induced by quantum defect of the lasing process could be reduced. For OPO crystal, by selecting proper pump source that can produce liner polarized fundamental wave to reduce the “waste” energy, as said previously, the thermal load of the OPO crystal could be improved. Furthermore, optimal design of the cavity could supply better mode overlap between the fundamental and signal waves, which would also improve the parametric conversion efficiency.

We studied the temporal characteristics using a digital phosphor oscilloscope (TDS 5052B, Tektronix, 500 MHz). The 1.5 μm pulses were detected by an InGaAs photodiode and the 3.5 μm pulses by an HgCdZnTe photoconductive detector. We measured the response parameter with a CW mode-locked 1,064 nm laser, which had a pulse width of around 40 ps. The result for InGaAs case was around 1 ns, and that of HgCdZnTe case was around 5 ns. Figure 4 gives the pulse widths (FWHM) with respect to the diode

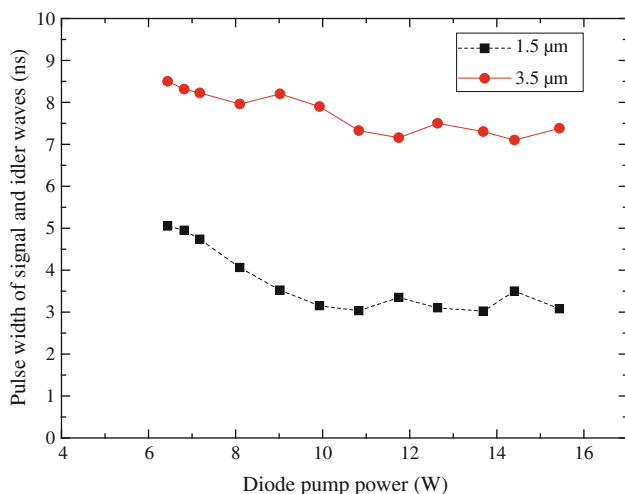


Fig. 4 Pulse widths with respect to the diode pump powers at 40 kHz

pump power at 40 kHz. It is noted that the pulse widths results in Fig. 4 were obtained from deconvolution of the recorded pulse shape and the equipment response function. Each point was obtained by averaging arbitrary ten experimental values. At the highest output power, the 1.5 and 3.5 μm pulse widths were measured to be 3.1 and 7.2 ns, respectively. This led to a peak power of 5.8 and 0.4 kW, respectively. In Fig. 5, we show the typical pulse shapes recorded from the oscilloscope. The upper one depicts the idler pulse and the lower one is signal pulse. From Figs. 3 and 4, we can see that the pulse widths of 1.5 μm laser were shorter than those of 3.5 μm laser. In singly resonant OPO, the cavity loss of the non-resonant wave is larger than that of the resonant wave. Larger cavity loss results in shorter photon lifetime and hence, short pulse width. Therefore, the signal pulse widths are shorter in our experiment.

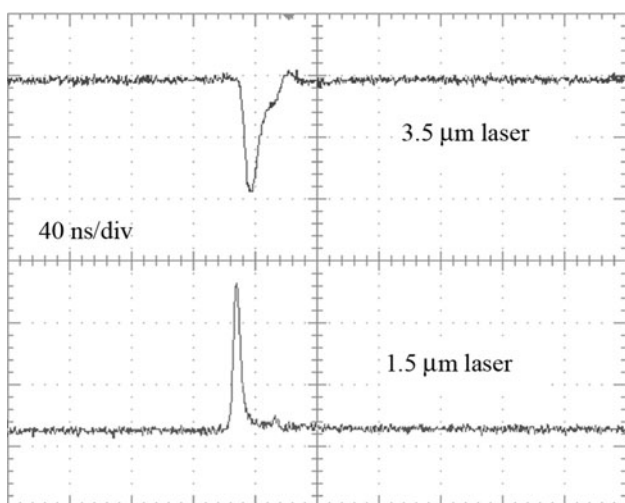


Fig. 5 Typical temporal shapes at the highest output power. The upper one is idler pulse and the lower one is signal pulse

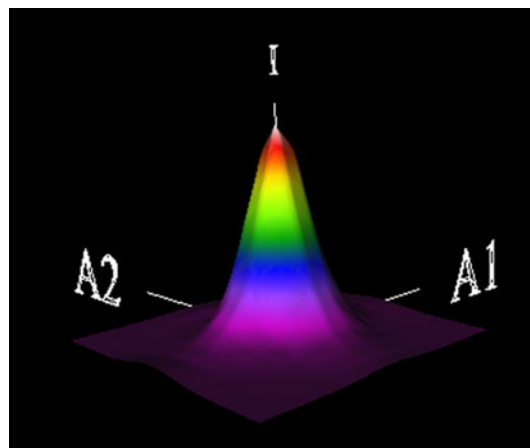


Fig. 6 Three-dimension beam profile of idler wave

The output beam profiles were monitored by a nano-scan beam analyzer and a precision linear stage (Zolix, Inc). By focusing the beam with a ZnSe lens ($f = 100$ mm), we measured the beam quality factors (M^2) for both signal and idler waves at the highest output power. The M^2 factors of the signal wave in horizontal and vertical directions were measured to be 3.7 ± 0.1 and 4.1 ± 0.1 , respectively. Those for idler wave were 1.1 ± 0.1 and 1.2 ± 0.1 . Particularly, compared with the previous works about signal-resonant KTA-OPO, the beam quality of the 3.5 μm laser was significantly improved in our experiment. Figure 6 gives the three-dimension beam profile of idler wave.

4 Conclusions

We have realized what are to our knowledge the first experimental results of idler-resonant KTA-OPO. With a diode pump power of 15.4 W, the idler output power was obtained to be 105 mW at 3,467 nm and the signal output power was obtained to be 720 mW at 1,535 nm. The conversion efficiency from diode to total OPO output power was 5.4 %. During the experiment, we found the pulse widths of the idler laser were wider than that of the signal laser. Moreover, a significant improvement of the beam quality was observed for the idler wave. Selecting more appropriate gain medium and optimizing the cavity design are expected to yield improved OPO performance.

Acknowledgments This work was supported by the National Natural Science Foundation of China (No. 60908010), Special Grade of China Postdoctoral Science Foundation (No. 201003632) and Independent Innovation Foundation of Shandong University, IIFSDU (No. 2009JC003).

References

1. K.L. Vodopyanov, F. Ganikhanov, J.P. Maffetone, I. Zwieback, W. Ruderman, *Opt. Lett.* **25**, 841 (2000)
2. R.F. Wu, K.S. Lai, H. Wong, W.-J. Xie, Y. Lim, E. Lau, *Opt. Express* **8**, 694 (2001)
3. F. Bai, Q.P. Wang, Z.J. Liu, X.Y. Zhang, X.B. Wan, W.X. Lan, G.F. Jin, X.T. Tao, Y.X. Sun, *Opt. Express* **20**, 807 (2012)
4. X.L. Dong, B.T. Zhang, J.L. He, H.T. Huang, K.J. Yang, J.L. Xu, C.H. Zuo, S. Zhao, G. Qiu, Z.K. Liu, *Opt. Commun.* **282**, 1668 (2009)
5. J.G. Miao, J.Y. Peng, B.S. Wang, H.M. Tan, *Appl. Opt.* **47**, 4287 (2008)
6. K. Zhong, J.Q. Yao, D.G. Xu, J.L. Wang, J.S. Li, P. Wang, *Appl. Phys. B* **100**, 749 (2010)
7. Q.B. Sun, H.J. Liu, N. Huang, C. Ruan, S.L. Zhu, W. Zhao, *Laser Phys. Lett.* **8**, 16 (2011)
8. W.J. Sun, Q.P. Wang, Z.J. Liu, X.Y. Zhang, F. Bai, X.B. Wan, G.F. Jin, X.T. Tao, Y.X. Sun, *Appl. Phys. B* **104**, 87 (2011)
9. M. Ebrahimzadeh, P.J. Phillips, S. Das, *Appl. Phys. B* **72**, 793 (2001)
10. U. Ströbner, J.-P. Meyn, R. Wallenstein, P. Urenski, A. Arie, G. Rosenman, J. Mlynek, S. Schiller, *J. Opt. Soc. Am. B* **19**, 1419 (2002)
11. A. Gaydardzhiev, D. Chuchumishev, I. Buchvarov, D. Shumov, and S. Samuelson, *CLEO/Europe and EQEC 2011 Conference Digest* (2011)
12. A. Dergachev, D. Armstrong, A. Smith, T. Drake, M. Dubois, *Opt. Express* **15**, 14404 (2007)
13. W.X. Lan, Q.P. Wang, Z.J. Liu, X.Y. Zhang, X.B. Wan, F. Bai, H.B. Shen, G.P. Lv, G.F. Jin, X.T. Tao, *Laser Phys.* **22**, 656 (2012)
14. S. French, A. Miller, M. Ebrahimzadeh, *Opt. Quantum Electron.* **29**, 999 (1997)
15. J.D. Bierlein, H. Vanherzeele, A.A. Ballman, *Appl. Phys. Lett.* **54**, 783 (1989)
16. G.M. Loiacono, D.N. Loiacono, J.J. Zola, R.A. Stolzenberger, T. McGee, R.G. Norwood, *Appl. Phys. Lett.* **61**, 895 (1992)
17. S. Brosnan, R. Byer, *IEEE J. Quantum Electron.* **15**, 415 (1979)
18. K.S. Lai, R.F. Wu, P.B. Phua, *Proc. SPIE* **3928**, 43 (2000)